Materials Research Proceedings 41 (2024) 1559-1568 https://doi.org/10.21741/9781644903131-173

Effect of vibration frequency and amplitude on formability in rotational vibration-assisted incremental sheet forming (RV-ISF)

ZHU Hui[1,a], PENG Wenxuan[1,b] and LONG Hui[1,c*]

[1]Department of Mechanical Engineering, The University of Sheffield, Sheffield S1 3JD, UK

[a]hui.zhu@sheffield.ac.uk, [b]wx.dusk.peng@gmail.com, [c]h.long@sheffield.ac.uk

Keywords: Incremental Sheet Forming, Rotational Vibration, Material Formability

Abstract. Incremental sheet forming (ISF) is a flexible manufacturing process, potentially for producing small-batched and customized sheet products. To improve formability of hard-to-form materials, part surface finish and forming accuracy, the rotational vibration-assisted ISF (RV-ISF) has been developed by the University of Sheffield with the use of novel tool designs with either offsets or grooves on the tool surface to introduce both mechanical vibration and localized heating into the conventional ISF process (C-ISF). With the use of double-offset (T2) and four-groove (T4) tools in the experiments, this work studies the effects of tool design and tool rotational speed on sheet vibration amplitude and frequency, as well as their effects on forming temperature and force reduction and formability improvement. Results show that the sheet vibration amplitude is mainly influenced by the tool design, while the vibration frequency is affected by both tool design and rotational speed. RV-ISF with T4 shows greater material formability improvement of AA3003-O due to greater temperature rise and low-frequency-low-amplitude vibration. RV-ISF with T2 results in greater reduction of forming force because of the higher sheet vibration amplitude.

Introduction

Incremental sheet forming (ISF) is a flexible forming technology, with potentials for manufacturing small-batch or customized sheet parts to achieve considerable cost and time savings [1]. The advantages of the conventional ISF (C-ISF) include process flexibility, improved formability, reduced equipment requirements, short production cycle, low cost, and high material utilization. However, there are still some aspects requiring improvement to broaden the ISF application prospective, for instance, further enhancement of formability of hard-to-form materials for processing high-strength materials, improving part surface finish and forming accuracy.

To improve the material formability for manufacture of more complicated geometries, heat-assisted ISF (HA-ISF) processes were developed. As one variant of heat-assisted ISF processes, friction stir-ISF (FS-ISF) provided localized temperature rise without the need of using external heating devices, which led to the formability improvement, as reported by Otsu [2]. As the friction between forming tool and sheet material affected the surface roughness, Wang et al. [3] proposed a process window to achieve increased formability and maintain the surface quality of low-ductility aluminium alloys AA2024-T3 and AA5052-H31. Zhan et al. [4] developed a novel two-stage FS-ISF process for AA2024-T3 and AA6061-T4, and found that this process helped to improve the geometric accuracy, material ductility and strength because of forming the uniform grains, homogeneous and fine precipitates.

Efforts have also been made to develop ultrasonic vibration-assisted ISF (UV-ISF) for the reduction of forming force, improvement of surface finish and formability. Due to the effect of ultrasonic softening, Long et al. [5] found that materials with higher yield stress had greater forming force reduction because of greater stress superimposition and higher absorption of ultrasonic energy. Amini et al. [6] reported that the significant improvement of material formability of AA1050 sheets under ultrasonic assistance in ISF process. The results of Amini et al. [7] also

revealed that applying ultrasonic vibration together with tool rotation reduced the surface roughness significantly.

As concluded from literature, both FS-ISF and UV-ISF have some limitations. The parts formed by the FS-ISF usually have poor surface finish because of the friction effect between the tool and sheet at high temperatures. The limitation of the UV-ISF lies in the requirement of an ultrasonic generator for forming high-strength materials. By combining the features of FS-ISF and UV-ISF, the rotational vibration-assisted ISF (RV-ISF) has been proposed by the University of Sheffield [8] to take both advantages and avoid limitations of FS-ISF and UV-ISF by introducing friction heating and mechanical vibration with simple process setup and new tool designs. Long et al. [8] firstly proposed a novel type of rosette tools with three-grooves or four-grooves for developing a new ISF process of the RV-ISF to improve the material formability of a hard-to-form material of magnesium alloy AZ31B significantly. Lu et al. [9] firstly developed single-offset (T1) and double-offset (T2) vibration tools for generating both friction heating effect and mechanical vibration effect, which induced microstructure refinement of AZ31B magnesium alloy. Peng et al. [10] revealed that under the effect of low frequency and low amplitude vibrations by using the novel four-groove rosette tool (T4) design, the developed RV-ISF can improve the surface quality by reducing the formation of fish-scale surface texture.

Following the design of the double-offset tool T2 and the new four-groove rosette tool T4 for RV-ISF developed [8], this work analyses the vibration amplitude and frequency when employing different tool designs and rotational speeds. Experimental testing and finite element (FE) modelling are conducted to investigate the effect of the tool design and rotational speed on the forming temperature, forming force and formability of AA3003-O sheets.

Methods

RV-ISF tool designs

In this study, a hemispherical tool T0 was used in the C-ISF and FS-ISF to form sheet parts, while a double offset tool T2 and a four-groove rosette tool T4 were used in the RV-ISF, as shown in Fig. 1. In the C-ISF, the conventional tool T0 produces the localised material deformation at room temperature, and in the FS-ISF, localised temperature rise is produced by localised heat generation due to friction and plastic work. However, in the RV-ISF, the double offset tool T2 and four-groove rosette tool T4 introduce both localised temperature and sheet vibration because of the periodic contact and the loss of contact with the rotating tool. Different from T2, the advantages of T4 lie in greater contact area, frequent changes between contact and loss of contact status, with greater sheet vibration frequency and smaller vibration amplitude, and a possibility of producing higher temperature rise.

Experimental methods

AA3003-O sheets of 0.9 mm thickness were used for C-ISF, FS-ISF and RV-ISF tests. The sheets were cut into squared blanks with size of 150 mm × 150 mm. To test the capability and formability of RV-ISF, a hyperbolic truncated cone shape with varying drawing angle from 21° to 85° was designed and the toolpath was generated as shown in Fig. 2(c) and (d). Identical feed rate of 1000 mm/min and step size of 0.3 mm were applied for all tests. The summary of the ISF tests can be found in Table 1. T0, T2 and T4 tools were tested with different rotational speeds. For all the tests, machine oil was used as lubricant. The ISF tests were performed on a 3-axis CNC milling machine (XYZ 1060 HS) as shown in Fig. 2(a). During the tests, forming forces were recorded by a 3-axis force transducer (Kistler 9367C), forming temperature were recorded by an infrared thermal camera (FLIR T650sc), and the fracture depth was recorded by the machine controller. Considering the deformation in plane strain condition for ISF of truncated cone parts, the

equivalent fracture strain $\bar{\varepsilon}_f$ were calculated by Eq. (1) with the initial sheet thickness t_0 and the thickness at fracture t_f after tests.

$$\bar{\varepsilon}_f = \frac{2}{\sqrt{3}} \ln \frac{t_0}{t_f} \quad (1)$$

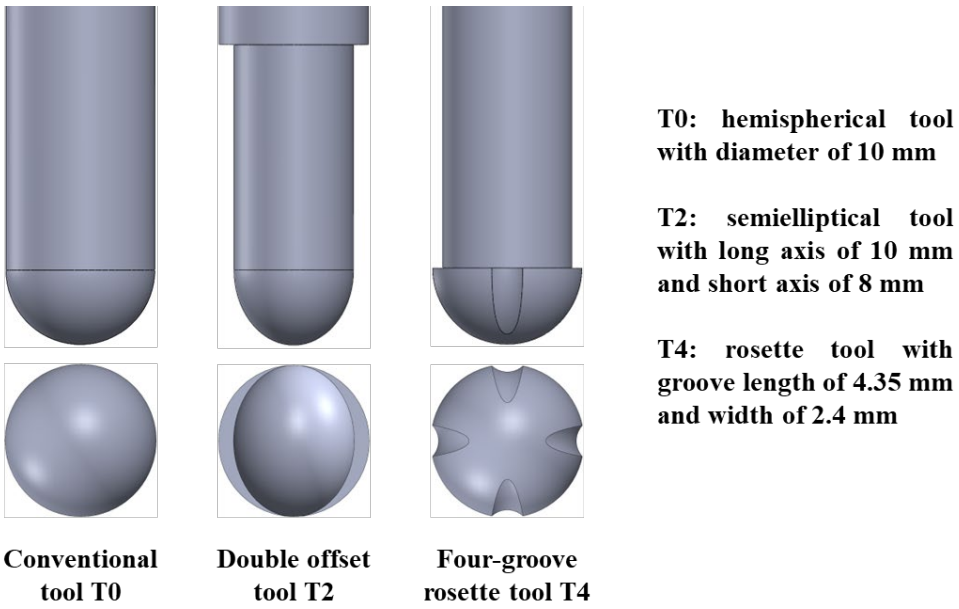

Fig. 1. Tool design: conventional tool T0, double offset tool T2 and four-groove tool T4.

Table 1. Experimental test parameters of C-ISF, FS-ISF and RV-ISF of AA3003-O sheets with hyperbolic truncated cone shape.

No.	Material	Sheet thickness [mm]	Tool design	Rotational speed [rpm]	Feed rate [mm/min]	Step size [mm]	Lubricant
1	AA3003-O	0.9	T0	0	1000	0.3	Machine oil
2	AA3003-O	0.9	T0	4000	1000	0.3	Machine oil
3	AA3003-O	0.9	T0	7000	1000	0.3	Machine oil
4	AA3003-O	0.9	T2	3000	1000	0.3	Machine oil
5	AA3003-O	0.9	T2	6000	1000	0.3	Machine oil
6	AA3003-O	0.9	T4	3000	1000	0.3	Machine oil
7	AA3003-O	0.9	T4	5000	1000	0.3	Machine oil
8	AA3003-O	0.9	T4	6000	1000	0.3	Machine oil
9	AA3003-O	0.9	T4	7000	1000	0.3	Machine oil

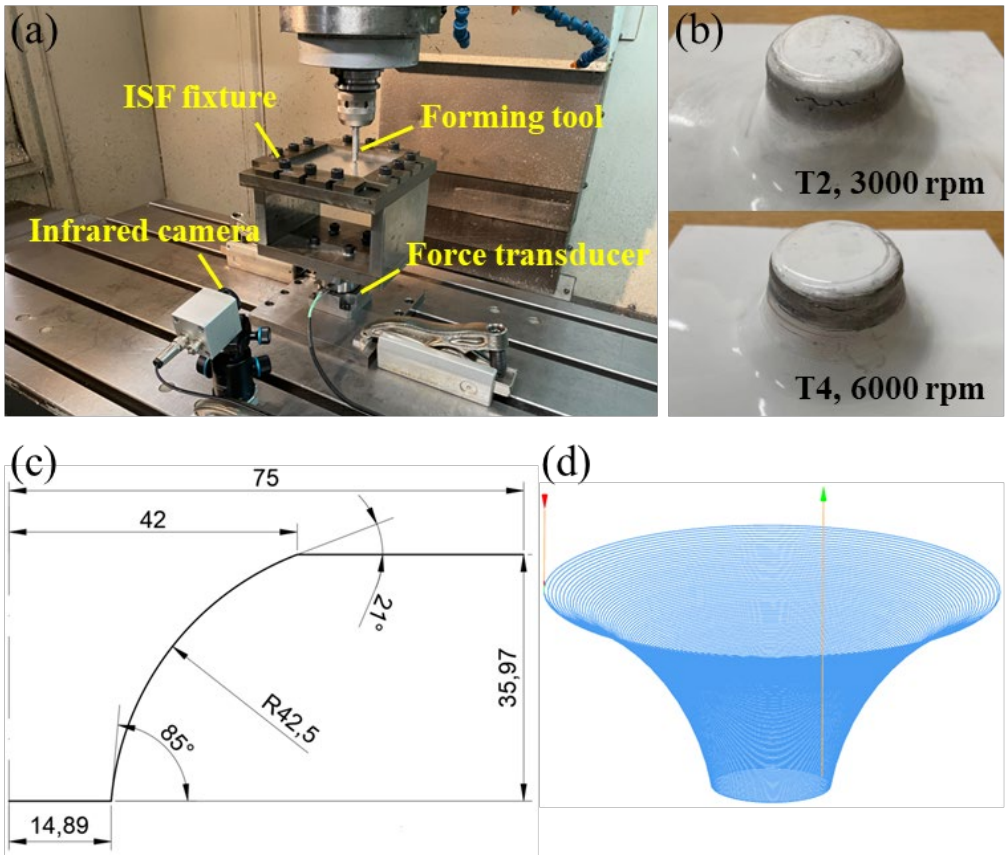

Fig. 2. (a) RV-ISF test setup; (b) RV-ISF formed hyperbolic truncated cone parts; (c) Dimensions of the designed hyperbolic truncated cone; (d) Generated toolpath.

Finite element (FE) modelling

FE simulation was conducted by using ABAQUS software to analyse the vibration frequency and amplitude of sheet material with the use of T2 and T4. Forming tools and a pre-shaped truncated cone part with a constant drawing angle of 50 ° and a forming depth of 30 mm were used in the FE model. After moving downwards for 0.3 mm, the forming tool T2 or T4 followed a circular toolpath, which was defined based on a fixed depth. The field output was requested at every 10^{-3} s to obtain the displacement data for calculation of vibration frequency and amplitude by fast Fourier transform (FFT). As the temperature effect was not considered in the vibration simulation, Johnson-Cook model without the temperature-related term was used for the material plasticity definition as given in Eq. (2):

$$\bar{\sigma} = \left(A + B\bar{\varepsilon}_{\mathrm{p}}{}^{n}\right)\left(1 + C\ln\frac{\dot{\varepsilon}}{\dot{\varepsilon}_{\mathrm{ref}}}\right) \tag{2}$$

where, $\bar{\sigma}$ is the equivalent stress, $\bar{\varepsilon}_{\mathrm{p}}$ is the equivalent plastic strain, $\dot{\varepsilon}$ is the strain rate, $\dot{\varepsilon}_{\mathrm{ref}}$ is the reference strain rate, A, B, n and C are model parameters. Table 2 gives the parameters for Johnson-Cook model and other material parameters. The coefficient of friction was set as 0.15. The deforming sheet was meshed with 8-node brick elements with reduced integration (C3D8R) and the forming tool was meshed with 4-node tetrahedral elements (C3D4). To achieve a balance between simulation accuracy and efficiency, the mass scaling was used to request a minimum time increment of at 10^{-5} s.

Table 2. Material parameters of AA3003-O [11] used in FE modelling of RV-ISF.

Johnson-Cook model	A (MPa)	B (MPa)	n	C
Value	42.97	180	0.21	0.00747
Other parameters	Density (kg/m^3)	Young's modulus (MPa)	Poisson's ratio	
Value	2790	72600	0.36	

Results and discussions

Analysis of vibration frequency and amplitude using FE simulation

In RV-ISF, the sheet vibration is resulted from the contact and loss of contact between forming tool and sheet surface. In theory, the reference vibration frequency can be calculated by the following equation:

$$f_{\text{ref}} = \frac{N \cdot S}{60} \tag{3}$$

where N is the number of tool offsets or grooves and S is the tool rotational speed. The calculated reference frequencies for T2 and T4 with 3000 rpm and 6000 rpm are listed in Table 3.

Table 3. Reference frequencies, simulated frequencies and amplitudes for T2 and T4 in RV-ISF.

Condition	Reference frequency	Simulated frequency	Simulated amplitude
T2, 3000 rpm	100 Hz	100 Hz	17.34 μm
		200 Hz	18.47 μm
		300 Hz	8.48 μm
T2, 6000 rpm	200 Hz	193.33 Hz	12.45 μm
		206.67 Hz	12.72 μm
		406.67 Hz	4.33 μm
T4, 3000 rpm	200 Hz	60 Hz	3.28 μm
		113.33 Hz	2.34 μm
		200 Hz	4.92 μm
T4, 6000 rpm	400 Hz	66.67 Hz	2.55 μm
		113.33 Hz	2.64 μm

The vibration frequency and amplitude of different tool designs at different tool rotational speeds were analysed by FE simulation. As shown in Fig. 3, the displacement data were obtained from the field output of the FE simulation. After adjusting the data with relative time and centralizing the displacement – relative time curve, the amplitude – frequency diagram was obtained by FFT as shown in Fig. 3(d).

Fig. 4 shows the simulated vibration frequencies and amplitudes of T2 and T4 with 3000 rpm and 6000 rpm, respectively. The peaks appearing in the amplitude – frequency diagrams are summarised in Table 3. For T2 tool, the simulated vibrations can be seen at 100 Hz and 200 Hz for 3000 rpm and 6000 rpm, respectively, which are the fundamental frequencies and are the same to the reference values. Harmonics can also be found at higher frequencies. For T4 tool with 3000 rpm, the simulated vibration can be seen at 200 Hz, the same as the reference frequency. However, the peak vibration by T4 tool with 6000 rpm from the FE simulation does not show the reference frequency, which should appear at 400 Hz. Both cases of using T4 with 3000 rpm and 6000 rpm predict small peaks at lower frequencies of around 66.67 Hz and 113.33 Hz, which may be resulted from the simulation error because mass scaling was used to reduce computational time.

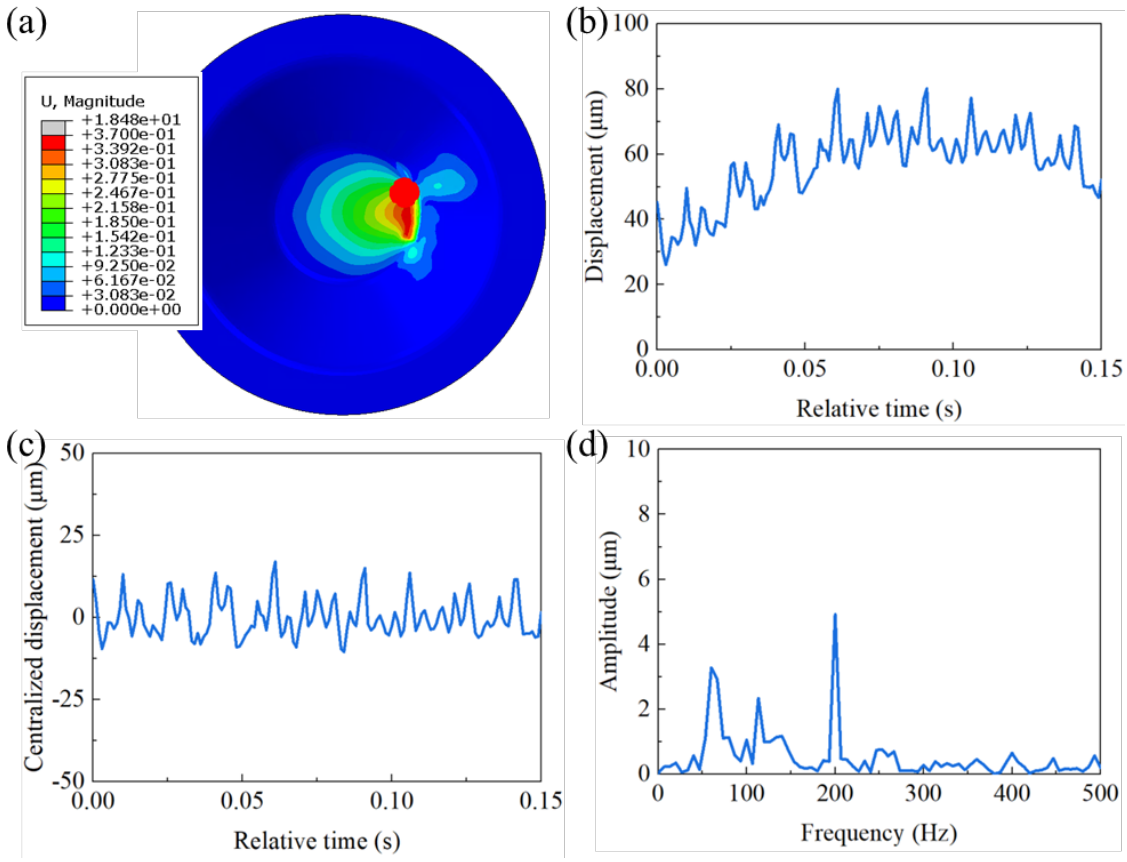

Fig. 3. Calculation process of vibration frequency and amplitude in the RV-ISF FE simulation of AA3003-O using T4 with 3000 rpm: (a) Displacement map; (b) Displacement – relative time curve; (c) Centralized displacement – relative time curve; (d) Amplitude – frequency diagram.

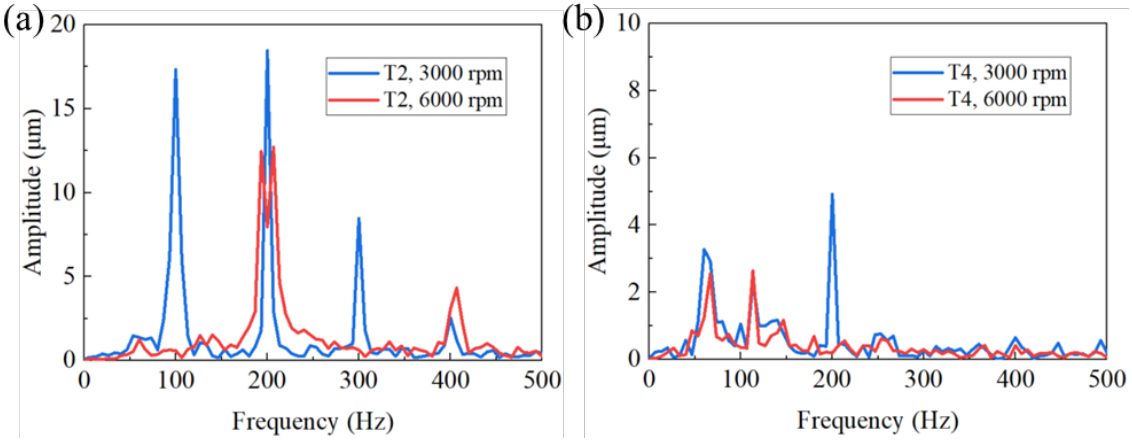

Fig. 4. Vibration frequencies and amplitudes of T2 and T4 with 3000 rpm and 6000 rpm from FE simulation results

Obviously, the increase of tool rotational speed leads to an increased sheet vibration frequency. It is also observed that for both T2 and T4, the increase of tool rotational speed results in the reduction of vibration amplitudes. Especially for T4, the higher frequency and amplitude from the FE simulation disappear at high rotational speed of 6000 rpm. The reason may be the insufficient

response time for the elastic recovery of sheet material at higher tool rotational speeds. By comparing the simulated amplitudes under the same rotational speed of 3000 rpm or 6000 rpm, or under the same vibration frequency of T2 with 6000 rpm and T4 with 3000 rpm, it is found that the vibration amplitudes produced by T4 is always smaller than that of T2.

Effect of tool design and rotational speed on forming temperature

As observed from Fig. 5, the rotation of both T2 and T4 tools can lead to temperature rise, resulted from the friction heat and plastic work. For all the cases with tool rotation, the forming temperature firstly increases to a peak value, and then keeps decreasing until the end of the process. The possible reason for the decreasing trend of forming temperature at later stage may be the reduced heat gain from friction due to the reduction of forming force at higher drawing angles. The measured forming temperature variations with different tools are shown in Fig. 5(a). With the same rotational speed of 3000 rpm or 6000 rpm, the RV-ISF with T4 tool has higher forming temperature than that with T2 tool, which mainly results from the larger contact area with T4 tool. The temperature difference between RV-ISF with T4 tool and T2 tool was much enlarged when higher rotational speed of 6000 rpm was used. For T4 tool, the effect of rotational speed on the forming temperature is depicted in Fig. 5(b). It is clearly shown that the increase of rotational speed has a positive effect on the temperature rise in the RV-ISF with T4.

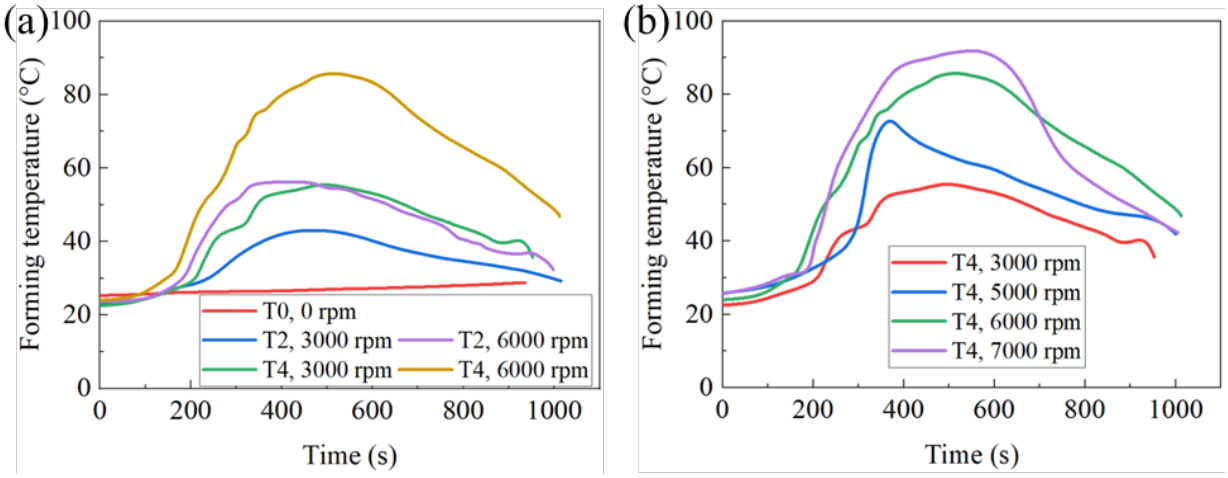

Fig. 5. Effect of (a) tool design and (b) rotational speed on the forming temperature from the experimental measurement.

Effect of tool design and rotational speed on vertical forming force

The effect of tool design on the vertical forming force of the RV-ISF is shown in Fig. 6(a). By comparing with the result of the C-ISF with the conventional tool T0, the sheet vibration induced by tool rotation of T2 and T4 leads to the significant reduction of the vertical forming force, and large force variations especially at the later stage. The force reduction is resulted from the easier dislocation activation under higher vibration energy density E_V, which is proportional to the square of vibration amplitude and frequency, respectively, as given by Eq. (4) [12]:

$$E_V = 2 \cdot \pi^2 \cdot \xi^2 \cdot f^2 \cdot \rho \quad (4)$$

where ξ and f are the vibration amplitude and frequency, respectively, and ρ is the material density. With the same rotational speed of 3000 rpm, the use of T2 is more effective in reducing forming force because T2 can provide larger vibration amplitude for the sheet material, as analysed

by FE simulation. With the same sheet vibration frequency, i.e., T4 with 3000 rpm and T2 with 6000 rpm, the effect of T2 for the forming force reduction is still greater than that of T4.

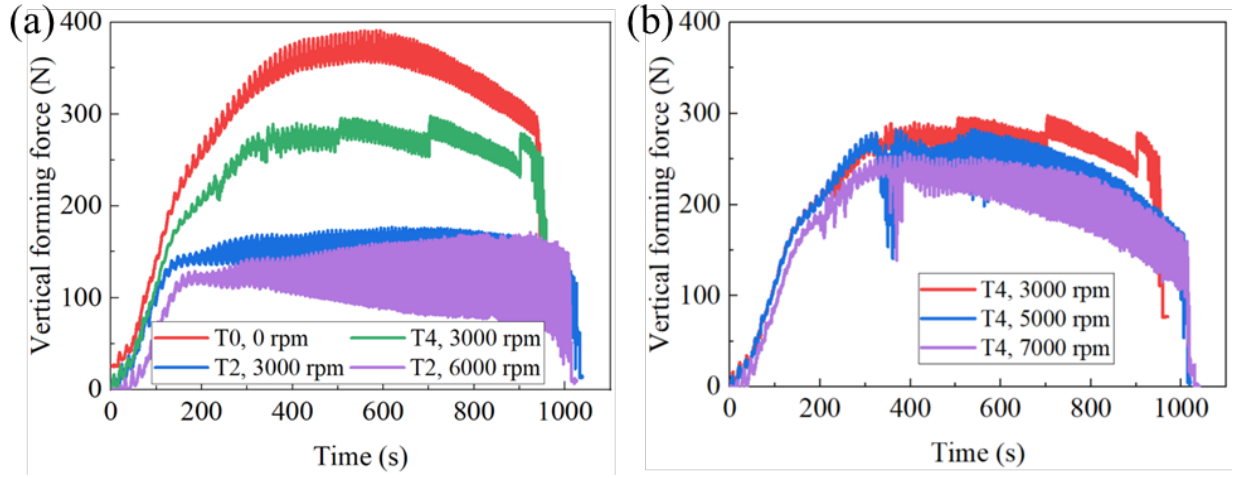

Fig. 6. Effect of (a) tool design and (b) rotational speed on the forming force reduction from the experimental measurement.

The effect of rotational speed on vertical forming force by using T4 is studied by comparing the force variation under different rotational speeds, as shown in Fig. 6(b). The vertical forming force is reduced with the increase of rotational speed or vibration frequency. The two possible explanations are: (1) the enhanced temperature rise caused by more friction heating at high rotational speeds; (2) the early dislocation activation due to higher vibration energy density with the increase of rotational speeds, as indicated by Eq. (4).

Effect of tool design and rotational speed on formability

The effects of tool design and rotational speed on the formability are shown in Fig. 7, in which fracture depth and equivalent fracture strain are used for comparison. By comparing the fracture depth and equivalent fracture strain of parts formed by T0, T2 and T4 at different rotational speeds, it is observed that the parts formed by T4 tool has achieved the highest formability. The reason may be that, compared with the temperature rise by T0 and the low-frequency-high-amplitude vibration with limited temperature rise by T2, T4 can provide both sufficient localized temperature rise and low-frequency-low-amplitude vibration, which may be useful for the improvement of material ductility.

By observing the fracture depth and equivalent fracture strain results by using T4, with the increase of rotational speed, the formability of the formed parts increases first but this is followed by a decreasing trend. The part formed by T4 has the highest formability when the rotational speed is 6000 rpm, and the highest equivalent fracture strain reaches 2.49. The reason for the initial increased formability is resulted from the temperature rise, increased vibration frequency and decreased vibration amplitude. The subsequent decreasing trend with higher rotational speeds may be that the sheet material is excessively softened and the deformation become unstable, so that fracture is initiated and propagated earlier.

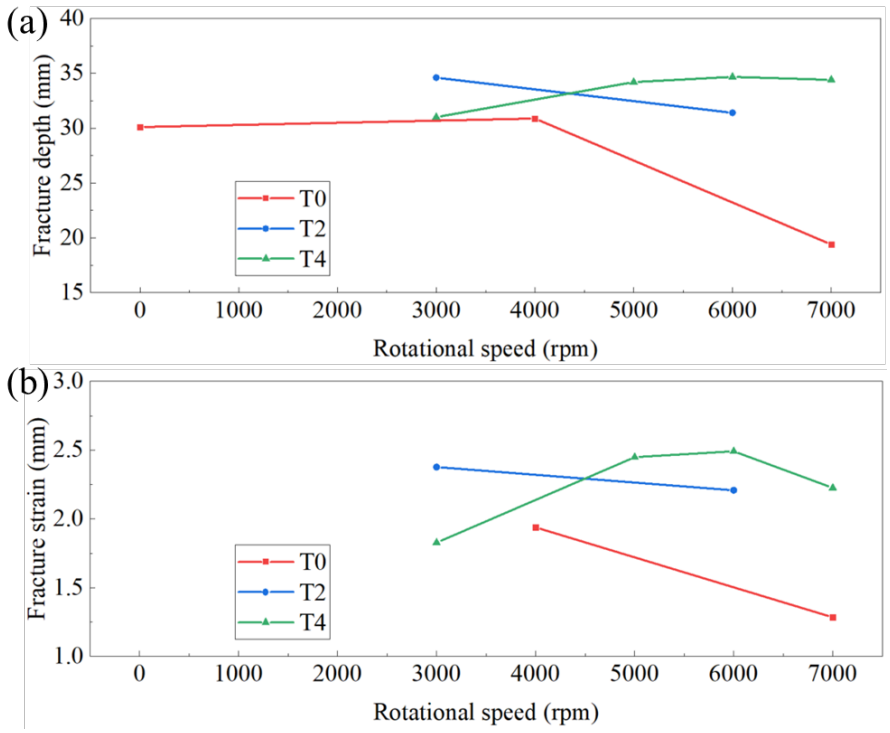

Fig. 7. Effect of the tool design and rotational speed on the (a) fracture depth and (b) equivalent fracture strain.

Conclusions

This work analyses the vibration amplitudes and frequencies under different tool designs and rotational speeds in the RV-ISF, and studies the effect of tool design and rotational speed on the forming temperature, forming force, and formability when forming AA3003-O sheets. The main conclusions may be drawn as below:

(1) The new design of four-groove rosette tool T4 can lead to the sheet vibration with low frequency and low amplitude, while the double-offset tool T2 causes low frequency and high amplitude vibrations. The increase of tool rotational speed leads to increasing sheet vibration frequency.

(2) Higher tool rotational speeds contribute to higher forming temperature increases, and the rotation of T4 leads to higher temperature rise than that by T2 because of larger contact area of T4.

(3) Greater reduction of the forming force can be achieved by using T2 than by T4 because of the higher vibration amplitude induced by T2; while the increasing rotational speeds of T4 result in smaller forming forces due to the higher temperature rise and vibration frequency.

(4) RV-ISF with T4 can improve the formability as compared with C-ISF with T0, FS-ISF with T0 and RV-ISF with T2, because of T4 producing higher temperature rise and low-frequency-low-amplitude vibration. Applying a rotational speed of T4 below a certain limit has positive effect on the formability improvement. For all the tools studied, the fracture depth and equivalent fracture strain start to decrease when the rotational speed applied is beyond a certain limit.

Acknowledgements

This work was financially supported by the UK Engineering and Physical Sciences Research Council (EPSRC) through project grants EP/W010089/1 and EP/T005254/1. The authors would like to acknowledge the contribution from Jamie Booth, an Engineering Team Leader of the Department of Mechanical Engineering, the University of Sheffield, for performing all experimental tests.

References

[1] J. R. Duflou, A.M. Habraken, J. Cao, R. Malhotra, M. Bambach, D. Adams, H. Vanhove, A. Mohammadi, J. Jeswiet, Single point incremental forming: state-of-the-art and prospects, Int. J. Mater. Form. 11 (2018) 743-773. https://doi.org/10.1007/s12289-017-1387-y

[2] M. Otsu, Friction stir incremental forming of aluminum alloy sheets, Proc. Metal forming (2010) 942-945.

[3] Z. Wang, S. Cai, J. Chen, Experimental investigations on friction stir assisted single point incremental forming of low-ductility aluminum alloy sheet for higher formability with reasonable surface quality, J. Mater. Process. Technol. 277 (2020) 116488. https://doi.org/10.1016/j.jmatprotec.2019.116488

[4] X. Zhan, D. An, J. Chen, A novel two-stage friction stir-assisted incremental sheet forming method for uniform microstructure and enhanced properties in aluminum alloys, Int. J. Mach. Tools Manuf. 180 (2022) 103928. https://doi.org/10.1016/j.ijmachtools.2022.103928

[5] Y. Long, Y. Li, J. Sun, I. Ille, J. Li, J. Twiefel, Effects of process parameters on force reduction and temperature variation during ultrasonic assisted incremental sheet forming process, Int. J. Adv. Manuf. Technol. 97 (2018) 13-24. https://doi.org/10.1007/s00170-018-1886-0

[6] S. Amini, A. Hosseinpour Gollo, H. Paktinat, An investigation of conventional and ultrasonic-assisted incremental forming of annealed AA1050 sheet, Int. J. Adv. Manuf. Technol. 90 (2017) 1569-1578. https://doi.org/10.1007/s00170-016-9458-7

[7] S. Amini, F. Nazari, M. Baraheni, A. H. Ghasemi, Investigating the effect of rotation speed and ultrasonic vibrations in the incremental forming process, Int. J. Adv. Design Manuf. Technol. 11(2018) 4 91-97.

[8] H. Long, W. X. Peng, Z. D. Chang, H. Zhu, Y. J. Jiang, Z. H. Li, New Rosette Tools for Developing Rotational Vibration-assisted Incremental Sheet Forming, Journal of Materials Processing Technology 118311 (2024). https://doi.org/10.1016/j.jmatprotec.2024.118311

[9] B. Lu, Z. Li, H. Long, F. Chen, J. Chen, H. Ou, Microstructure refinement by tool rotation-induced vibration in incremental sheet forming, Procedia Eng. 207 (2017) 795-800. https://doi.org/10.1016/j.proeng.2017.10.831

[10] W. Peng, E. Hurtado Molina, F. Solum, J. Booth, H. Long, Surface and Friction Characterisation of Rotational Vibration-Assisted Incremental Sheet Forming, in International Conference on the Technology of Plasticity (2023) Springer 756-765. https://doi.org/10.1007/978-3-031-41023-9_76

[11] A. Saulo, A. Carlos, E. Márcio, Numerical Study on Incremental Sheet Forming Applied on an Impact Attenuator Model, in 22nd International Congress of Mechanical Engineering (COBEM 2013) November 3-7, 2013 Ribeirão Preto, SP, Brazil, (2013) ABCM 6077-6086.

[12] A. Pierce, Basic linear acoustics, Springer Handbook of Acoustics, (2007) 25. https://doi.org/10.1007/978-0-387-30425-0_3